ORIGINAL RESEARCH

Investigating Sacroplasty: Technical Considerations and Finite Element Analysis of Polymethylmethacrylate Infusion into Cadaveric Sacrum

C.T. Whitlow
S.K. Yazdani
M.L. Reedy
S.E. Kaminsky
J.L. Berry
P.P. Morris

BACKGROUND AND PURPOSE: Sacroplasty is not as routinely performed as vertebroplasty, possibly due to technical challenges and the paucity of data regarding subsequent outcomes. The first goal of the present investigation was to describe a technique for sacroplasty that facilitates safe needle placement and polymethylmethacrylate (PMMA) extrusion. The second goal was to perform finite element analysis (FEA) by using a geometric model of sacral fracture to identify mechanical outcomes of sacroplasty.

MATERIALS AND METHODS: Sacroplasty was performed on fresh pelvis specimens (n = 4) under biplane fluoroscopy. Cadavers were imaged via CT before and after sacroplasty and volume rendered to examine needle placement and PMMA extrusion. The volume-rendered CT data were then used to generate geometric models of the intact, fractured, and cement-augmented fractured sacrum for comparison by using FEA.

RESULTS: CT data demonstrate that safe injection needle placement and PMMA delivery may be facilitated by orienting the needle parallel to the L5-S1 interspace and ipsilateral sacroiliac joint, then targeting the superolateral sacral ala within an area bounded by a line lateral to the posterior foraminal openings and a line superimposed on the medial edge of the sacroiliac joint. FEA revealed that simulated sacroplasty decreased maximal principal stress at the point of sacral fracture propagation by 83% and fracture gap micromotion by 48%.

CONCLUSION: Sacral landmarks can be used to place PMMA safely where sacral fractures occur. FEA suggests that sacroplasty may decrease fracture-associated mechanical stress and micromotion, which may contribute to patient reports of decreased pain and increased mobility postsacroplasty.

As the population of the elderly grows during the next decade, the prevalence of insufficiency fractures secondary to osteoporosis and osteopenia will dramatically increase. Sacral insufficiency fractures represent a relatively common variant of such injuries that are associated with severe and functionally debilitating pain.[1,2] Conventional therapy for sacral fractures involves the administration of analgesics of varying efficacy and, in some cases, prolonged bed rest.[3-5] Sacroplasty, a variant of vertebroplasty, is a minimally invasive percutaneous procedure that has recently been described for the treatment of sacral insufficiency fractures.[6-8] Although sacroplasty is a procedural extension of vertebroplasty, it is not as routinely performed, despite the common occurrence of sacral insufficiency fractures.[7,8] This may be in part due to the lack of data regarding postprocedural benefits and outcomes, as well as technical challenges involved in performing the procedure, including injection needle placement and polymethylmethacrylate (PMMA) extrusion that avoids neural foramina impingement and soft-tissue compromise.

Although no formal controlled prospective randomized trials of sacroplasty have been conducted, retrospective investigations have demonstrated significant self-reported decreases in pain and improvements in the ability to ambulate and perform various activities of daily living postprocedure[6-9] (C.T. Whitlow, unpublished data, 2006). No studies to date, however, have investigated potential mechanisms for these effects. Although a role for the placebo effect cannot be underestimated, one plausible hypothesis for the apparent clinical efficacy of sacroplasty is that PMMA stabilizes the fracture by attenuating mechanical stress at the fracture site and decreasing fracture gap micromotion. This proposed mechanism for clinical improvement, however, would likely be difficult to evaluate in an in vivo model. As such, 1 viable way to test this hypothesis is with finite element analysis (FEA). FEA is an engineering method that has been used to evaluate the mechanical properties of bone in 3D geometric models.[10-14] This method has been previously applied to a limited nonfractured sacral model, demonstrating mechanical properties of PMMA in intact bone.[14] FEA is performed by dividing a 3D graphic object into smaller elements and assigning mechanical properties and loads to the elements via precise mathematic equations. The equations can then be solved for resultant deformation and maximal principal stress.

The first goal of the present study was to confirm a technique for sacroplasty that facilitates safe needle placement and

Received August 12, 2006; accepted after revision October 30.

From the Division of Radiologic Sciences, Department of Radiology (C.T.W., M.L.R., S.E.K., P.P.M.) and the Department of Biomedical Engineering (S.K.Y., J.L.B.), Wake Forest University School of Medicine, Winston-Salem, NC.

This work was supported by Parallax Medical Inc Research Grant (S.K.Y., M.L.R., S.E.K., J.L.B, P.P.M.) and the National Institutes of Health, National Research Service Award MD/PhD Predoctoral Fellowship Grant # F30 DA05911 (C.T.W.).

Paper previously presented at: Annual Meeting of the Radiological Society of North America, November 28–December 3, 2004; Chicago, Ill; and as part of a special focus session topic, November 27–December 2, 2005, Chicago, Ill.

Please address correspondence to P. Pearse Morris, MB, BCh, Division of Radiologic Sciences, Department of Radiology, Wake Forest University School of Medicine, 2nd Floor, Meads Hall, Medical Center Blvd, Winston-Salem, NC 27157; e-mail: pmorris@wfubmc.edu

DOI 10.3174/ajnr.A0500

PMMA extrusion by using volume-rendered 3D reconstructions of CT data following sacroplasty in cadaveric pelvic specimens. A second goal of the study was to use the volume-rendered CT data to generate a geometric model of the intact, fractured, and cement-augmented sacrum for comparison by using FEA to evaluate potential mechanical benefits and outcomes of sacroplasty.

Materials and Methods

Cadaveric Tissue. Fresh pelvis specimens ($n = 4$) were harvested from nonembalmed human cadavers (2 women and 2 men; age range at time of death, 69–87 years; mean age, 78 years). The cadaveric specimens were obtained according to the policies and procedures of the Wake Forest University School of Medicine. All pelvic tissue was obtained from individuals with no known significant pathologic process involving the pelvis, other than osteoporosis, and no history of pelvic surgery or fracture.

Sacroplasty Technique. Pelvis specimens were positioned in a prone orientation and biplane fluoroscopy manipulated to visually guide an 11-gauge needle into the sacral ala. PMMA was then infused by using a Parallax injection system (EZflow Cement Delivery System, Parallax Medical, Sunnyvale, Calif).

Image Acquisition. All cadavers were imaged in the supine position with a helical CT scanner (LightSpeed Pro16, GE Healthcare, Milwaukee, Wis) before and after sacroplasty. Axial CT images were obtained by using the following parameters: 0.625-mm section thickness, 1.375:1 pitch, 120 kV, 540 mA, no gantry tilt, 20 display FOV, and bone reconstruction algorithm. The CT images were then processed by using an Aquarius imaging workstation running TeraRecon software (TeraRecon, San Mateo, Calif) for 3D volume rendering. In the present study, 3D reconstructions of the pelvis were generated with a transparent-bone volume-rendering protocol bundled within the software package (TeraRecon).

FEA. 3D reconstructions of the cadaveric CT data were exported onto a PC workstation, and Patran software (MSC Software, Costa Mesa, Calif) was used to perform finite element modeling (FEM) and FEA. For a comprehensive technical description of FEM and FEA, please see the methods of Anderson and Cotton.[14] Briefly, the CT data were initially used to construct a geometric FEM of the hemipelvis, consisting of individual elements interconnected by a meshwork of discrete points called nodes (Fig 1*A*). Specifically, 8-node brick elements were used in this model, which incorporated 25,000 nodes. Convergence testing showed that further mesh refinements beyond this number of nodes resulted in solutions to displacement differing by less than 2%. The system of elements and nodes was assigned elasticity parameters and material properties of bone on the basis of the densitometric data from CT, which was calibrated with densitometric phantoms of known attenuation. Hounsfield units are based on density-dependent attenuation of x-ray beams, the values of which are related to cancellous bone elasticity through statistical regression analysis by the relationship $E = 0.06 + 0.9^{*}r^2$, where E represents Young's modulus in MPa. Cortical bone elastic modulus was related through the regression equation $E = -6.142 + 0.014r$. The estimated values of elastic modulus are an order of magnitude higher for cortical bone (17 GPa). Thus, we assigned a uniform elasticity to the cortical shell and ignored the structural contribution of cancellous bone since the cortex carries the load. To simulate a sacral insufficiency fracture, we applied a 1-mm sacral crack to the intact FEM of the hemipelvis (Fig 1*B*). The sacroplasty intervention was modeled as a 3-mL column of PMMA within the fracture, oriented horizontally in the anteroposterior direction for the purpose of bridging the fracture gap. The elastic modulus for PMMA was defined as 2.7 GPa.[16] FEA was then conducted to evaluate changes in maximal principal stress following several simulations by using the constructed geometric FEM.

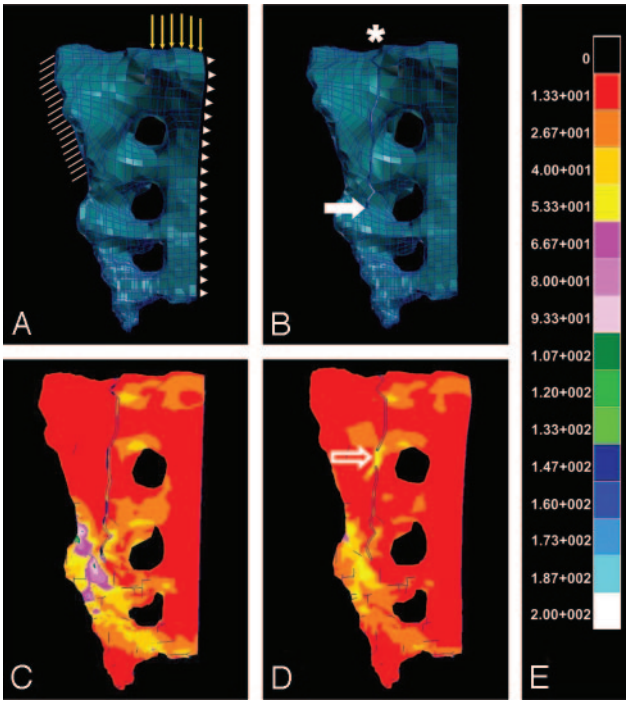

Fig 1. Intact (*A*) and fractured (*B*) FEMs of a hemisacrum are shown, which were constructed by using densitometric CT data from a single imaged cadaveric pelvis. In the models (*A, B*), a system of individual elements interconnected by a meshwork of discrete nodes has been assigned elasticity parameters approximating that of bone. Boundary and loading conditions applied to the intact sacral fracture and cement-augmented sacral fracture models are demonstrated (*A*). Hatch marks (*A*) represent boundary conditions that were applied to simulate anchoring of the sacrum at the sacroiliac joint. Yellow vector lines (*A*) indicate loading conditions, which were defined as a 35-kg force, approximating one half of body weight above the first sacral vertebra. Arrowheads (*A*) demonstrate the sagittal plane along which movement could occur in a 1-legged-stance paradigm. An asterisk and solid arrow (*B*) indicate sacral fracture origin and the point of fracture propagation, respectively. Color-coded transformation of FEA data demonstrates the amount of maximal principal stress experienced by the hemisacrum after the application of a 35-kg load, both before (*C*) and after (*D*) fusion at a point along the fracture (*open arrow*) designed to simulate sacroplasty. Each color represents kilopascals of maximal principal stress according to the calibration scale provided (*E*), with red corresponding to the lowest and white corresponding to the highest levels of maximal principal stress. Note that the point of fracture fusion (*open arrow, D*) appears to subsume a portion of the stress generated by the 35-kg load, thereby attenuating maximal principal stress that surrounds the site of fracture propagation, as compared with the prefusion model (*C*).

An initial simulation was conducted in which a 35-kg load, representing approximately one-half body weight, was assigned to the intact and fractured model of the hemipelvis. This distributed load was applied to the nodes representing the superior endplate of the first sacral vertebral body (Fig 1*A*). Two subsequent simulations applied this load to the fractured model of the hemi-pelvis following fusion at 2 separate points along the sacral fracture, respectively. The initial point of fusion corresponded to the optimal sacral area for injection, as determined from the CT analysis of sacroplasty in cadavers (Figs 1*D* and 2*C*, *-D*). The subsequent point of fusion was approximately 3 cm below the initial site, relatively more distal to the fracture origin. A final simulation was conducted to query for changes in fracture gap micromotion following sacroplasty at the proposed optimal injection site. In this simulation, single nodes on each side of the sacral fracture were selected near the point of fracture propagation, and internodal

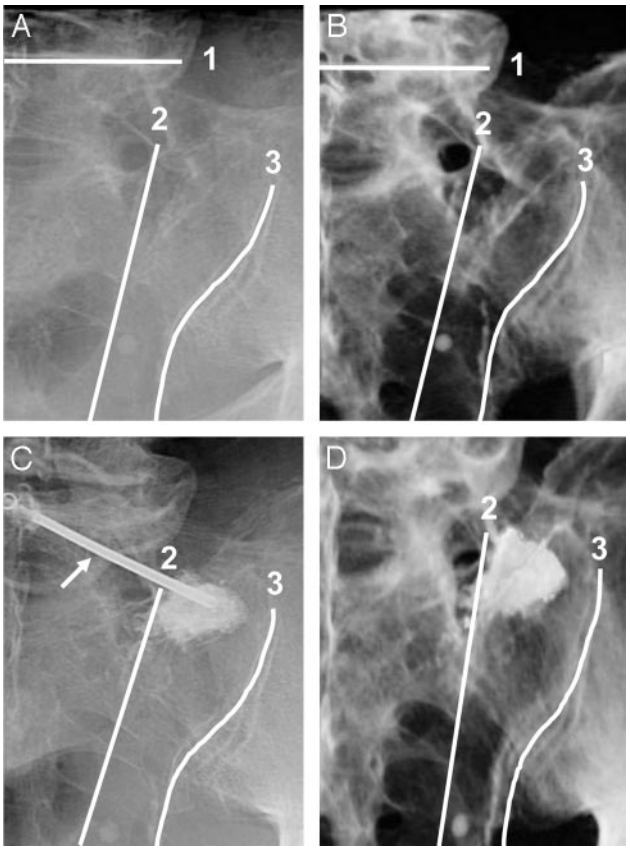

Fig 2. Fluoroscopic (*A, C*) and corresponding volume-rendered 3D reconstructions of CT images (*B, D*) of a hemisacrum from a single cadaveric pelvis, demonstrating anatomic landmarks for needle placement (*arrow* in image *C* indicates needle) and PMMA injection before (*A, B*) and after (*C, D*) sacroplasty. The sacrum is shown in a left posterior oblique orientation (*A–D*), with the beam manipulated parallel to the L5-S1 disk space[1] and ipsilateral sacroiliac joint.[3] Fluoroscopy (*C*) and CT (*D*) demonstrate PMMA within the superior-lateral sacral ala in an area bounded by the following: first, a line connecting the lateral edge of the posterior foraminal openings,[2] and second, a line superimposed on the medial edge of the sacroiliac joint.[3]

distance was measured after the 35-kg load was applied pre- and postsacroplasty.

Results

CT Data. The volume-rendered CT data provide high-resolution anatomic detail of the neural foramina and other bony structures of the sacrum before and after sacroplasty, which are not as apparent with fluoroscopic imaging (Fig 2). On the basis of examination of the 3D CT reconstructions, several landmarks were identified that appear to facilitate injection of PMMA, avoiding sacral foramina and soft tissues of the pelvis.

The first landmarks aid initial fluoroscopic orientation and needle placement. Needle access is nearly perpendicular to the dorsal surface of the sacrum when biplane fluoroscopy is manipulated to provide a left posterior oblique orientation of the pelvis that is parallel to the L5-S1 disk space and the ipsilateral sacroiliac joint (Fig 2). In the rostral-caudal pelvic axis, the next landmark corresponds to the most superior sacral foramen adjacent to the superolateral segment of the sacral ala. Injecting PMMA into the superolateral segment of the sacral ala, parallel or rostral to the most superior foramen, decreased the likelihood of PMMA encountering the inferior-oblique foraminal path (Figs 2 and 3). Furthermore, this superolateral segment of the sacral ala is also a relatively thick region of sacral bone. Targeting this area minimized the risk of the needle traversing too far and allowing cement extrusion into adjacent soft tissues.

In the medial-lateral pelvic axis, the next landmark corresponds to an area bounded by the following: first, a relatively straight line connecting the lateral edge of the posterior foraminal openings, and second, a line superimposed on the medial edge of the ipsilateral sacroiliac joint (Fig 2). Using these medial-lateral landmarks for injection into the superolateral segment of the sacral ala provided additional guidance to avoid soft-tissue and foraminal compromise. Because the anterior and posterior foraminal openings are somewhat superimposed in the left posterior oblique view of the sacrum, preventing cement from crossing the lateral foraminal line also prevented cement from spilling into the foramina. Avoidance of the line superimposed on the medial edge of the ipsilateral sacroiliac joint decreased the likelihood of cement extrusion into this joint space and subsequently tracking into soft tissues of the pelvis. Interestingly, injections that spread beyond the area of the superolateral sacral ala, bounded by the foraminal landmark, not only were observed to extravasate into the foramen but also increased the risk of distal cement embolization into the intravascular space (Fig 3).

FEA. When the intact and fractured sacral models (Fig 1*A*, -*B*) were compared following the application of a 35-kg load, FEA revealed a 99% increase in maximal principal stress (1.5 kPa in the intact and 156.2 kPa in the fractured sacral model) at the point of fracture propagation (Fig 1*C*). Maximal principal stress was attenuated by 83% (156.2-kPa prefusion versus 27.3-kPa postfusion) after simulated fusion of the fracture in an area consistent with the optimal sacroplasty injection site, relatively proximal to the origin of the fracture (Fig 1*D*). In contrast, maximal principal stress was attenuated by only 56% (156.2-kPa prefusion versus 56.2-kPa postfusion) after simulated fusion of the fracture in an area relatively more distal to the origin of the fracture and inferior to the proposed optimal sacroplasty injection site.

A final simulation was conducted to investigate micromotion of the fracture after sacroplasty was modeled at the proposed optimal sacroplasty site. Distance across the fracture was decreased by 48% (22.3-μm prefusion versus 11.6-μm postfusion) after simulated sacroplasty (Fig 4).

Discussion

This study demonstrates useful anatomic landmarks within the sacrum that facilitate safe needle placement and cement extrusion. This study also presents data from an FEA of a mechanical model of sacral fracture that demonstrate attenuation of maximal principal stress and micromotion following simulated fracture fusion, suggesting that this computational engineering method may be a valuable tool for investigating the biomechanics of sacroplasty.

Injection of PMMA into bone has been most extensively described in the context of vertebroplasty.[17-25] Such injections have been demonstrated in the literature to be safe for the treatment of vertebral insufficiency fractures.[20-22,25] Serious complications of vertebroplasty include cement extrusion into the vertebral foramina and venous circulation, resulting in nerve root compression and pulmonary embolism, respec-

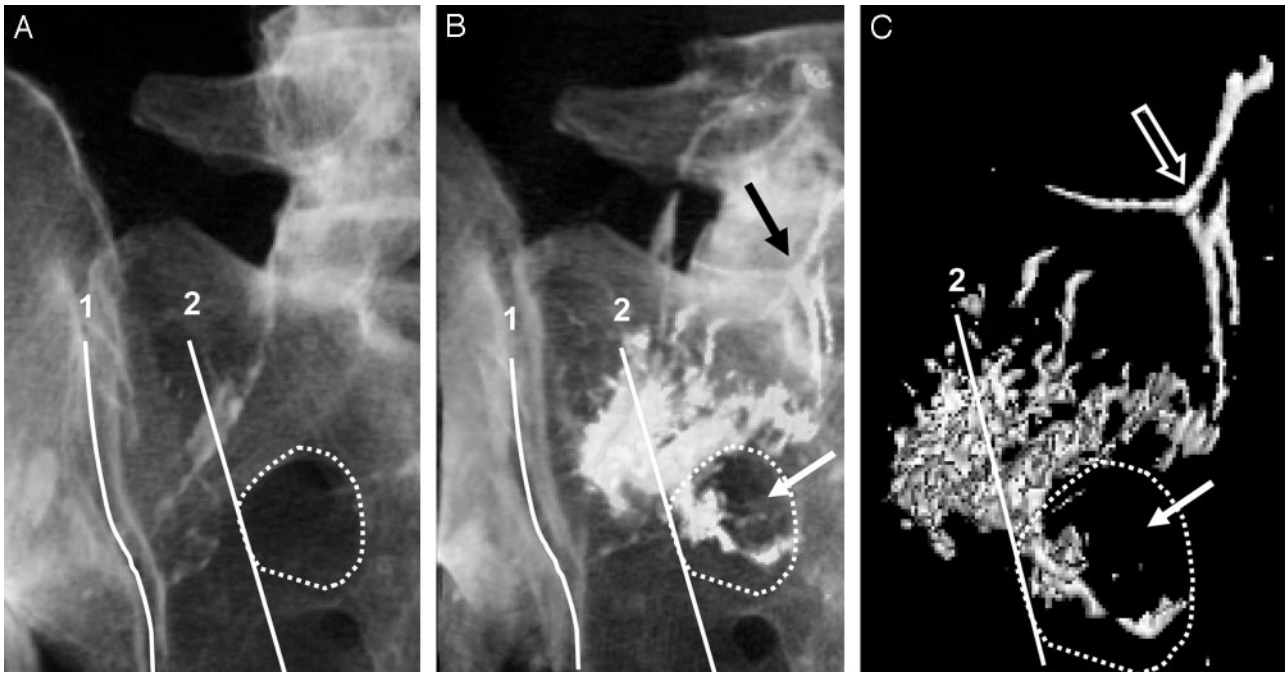

Fig 3. 3D reconstructed CT images (*A–C*) of a hemisacrum from a single cadaveric pelvis are shown in a left posterior oblique orientation. Anatomic landmarks used for injection overlie the sacrum and correspond to the following: first, a line superimposed on the medial edge of the sacroiliac joint,[1] and second, a line connecting the lateral edge of the posterior foraminal openings.[2] A dotted line demonstrates the outline of the most superior sacral foramen. Note that PMMA spreads beyond the foraminal landmark[2] and is appreciated within the sacral foramen (*white arrow*) and intravascular space (*black arrow*, *B*). Additional reformatting of the CT images (*C*) reveals the isolation of PMMA attenuation from sacral bone and more clearly shows PMMA tracking beyond the posterior foraminal landmark[2] into the sacral foramen (*solid arrow*) and intravascular space (*open arrow*).

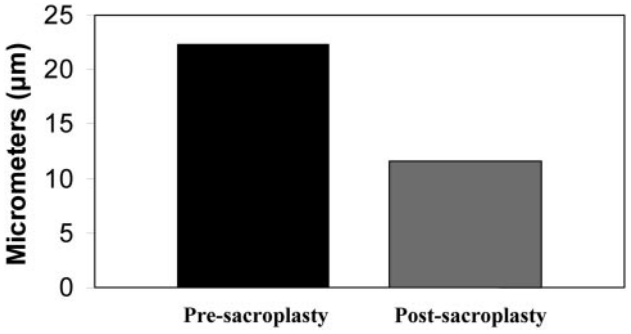

Fig 4. The effect of simulated sacroplasty on fracture gap micromotion in an FEM of the fractured hemisacrum is shown. In this simulation, single nodes on each side of the sacral fracture are selected near the point of fracture propagation and internodal distance measured after the application of a 35-kg load pre- and postsacroplasty. Fracture-gap micromotion is decreased by 48% after simulated sacroplasty, as compared with the nonfused fractured sacrum.

tively, among other complications.[23,26] Extrusion of cement into the sacral foramina and vascular circulation is also of concern when performing sacroplasty. Of particular difficulty in this regard is navigating the relatively complex anatomy of the sacrum. It is possible that such technical challenges encountered in this context and associated procedural risks have prevented some operators from performing sacroplasty. The anatomic landmarks identified in the present study may increase the ease and safety of sacroplasty, thereby increasing operator comfort level. Increased operator comfort level may lead to more routine application of this procedure. Indeed, key landmarks and technical protocols have been identified for vertebroplasty that have likely contributed to its relatively routine application.[21,27]

The present study was conducted by using cadaveric tissue specimens to facilitate experimentation with the sacroplasty procedure and to avoid risk to patients. As such, there are limits to the extrapolation of the present anatomic data to living tissue. First of all, the data were generated by using only 4 cadaveric specimens, which limits the ability to indiscriminately apply the findings to all patients. Anatomic variants and complex fracture patterns, for example, may require revision and modification of the described techniques. Given the lack of blood flow in cadaveric tissue, we believe the present study may under-represent the risk of intravascular compromise and cement embolization. Cement embolization may have been more apparent in the setting of vigorous blood flow in an intact living sacrum. Despite the lack of blood flow in the cadaveric tissue, intravascular cement compromise was seen when PMMA injection extended outside the described medial-lateral foraminal landmark (Fig 3). The extent of this embolization in perfused tissue is unknown. PMMA dispersion in cadaveric bone may also differ from that of living bone secondary to cadaveric tissue decomposition. The extent of tissue decomposition in the present study was limited, however, due to appropriate storage of the sacral specimens in refrigeration units and given that the specimens received sacroplasty less than 48 hours after the demise of the tissue donors. Despite these limitations, the described landmarks have been applied in more than 15 sacroplasty cases, with no associated complications (P.P.M., personal communication, July 1, 2006).

Anatomic landmarks and protocols for performing sacroplasty will likely evolve and be refined with time as more procedures are conducted. Additional techniques will also continue to be developed, such as the recently described long-axis injection technique, which will provide various procedural

options that may be more suitable for different patients and interventionalists.[28] Furthermore, the increased use of CT and CT-fluoroscopic guidance may provide improved anatomic detail with which to apply such landmarks.[29]

The use of FEA to investigate the effects of stress on bone was first described in the orthopedic literature in the early 1970s.[30] Advances in FEA have allowed the study of more complex questions relating to microstructural bone mechanics, adaptation of bone after damage, and optimal design of orthopedic implants.[31] In particular, FEA has been applied to the study of vertebroplasty to refine the procedure (eg, where to inject PMMA and the optimal amount to inject), study its effects on adjacent vertebrae, and study the material properties of bone cement used in vertebroplasty.[32-37] Similar FEA investigations would likely yield important data that would further improve the safety and efficacy of sacroplasty.

FEA has several strengths for investigating the mechanical properties of sacroplasty. FEA can reveal regions of a structure that are prone to fail due to excessive stress and can help determine design modifications to bolster the structure, thus reducing the risk for mechanical failure.[31] Unlike in vivo mechanical testing of cadaveric specimens, FEA allows the control of numerous parameters, such as bone attenuation, fracture severity, and PMMA use (eg, volume, placement, and material properties) without the requirement for fresh tissue to test each permutation.[31]

In the present investigation, the model geometry and bone-material properties were derived from a real human sacrum. As such, the model and FEA simulations describe trends in mechanical behavior following an interventional procedure, which approximates that of sacroplasty in fractured living sacral bone. The present FEA data, however, have important limitations that must be noted. The precise elasticity of sacral bone is not known and could only be estimated on the basis of the known relationship of bone attenuation, as measured by CT and bone elasticity.[15] The model of the hemipelvis used for this investigation incorporated limited anatomic data and isotropic material properties. The pelvis was modeled as a cortical shell, which did not account for the complex network of trabecular bone. This was justified because cortical bone carries most of the load and does so especially in the case of osteoporotic trabecular bone. However, because a volumetric model was not used, different mechanical properties regarding the bone attenuation measured for each element could not be assigned. This limitation of the model could affect fracture gap micromotion before and after fusion and, therefore, bias the results. Nevertheless, we conclude that the relative attenuation in fracture gap micromotion due to a sacroplasty intervention would be similar whether or not volumetric elements were present. The sacroplasty intervention was modeled as a small column of PMMA oriented horizontally in the anteroposterior direction for the purpose of bridging the fracture gap. This is a highly idealized distribution of bone cement, yet it emphasizes the fact that very little cement is needed to achieve fracture stabilization. It has been estimated that the hip and sacroiliac joint experience 3–4 times more force during walking than during passive standing.[38,39] It is, therefore, likely that force and maximal principal stress experienced at a site of sacral fracture propagation, as well as sacral gap micromotion, would be significantly higher during the more rigorous loading conditions of walking than the passive standing conditions modeled in the present study.

The model did not account for increased dynamic loading of material viscoelasticity. Stress and strain measured in the present model, however, would be expected to increase in a predictable manner as loading parameters were increased. The precise loading conditions required for failure of the sacral gap fusion modeled in the present study, however, are unknown. Indeed, future FEA studies would be useful to address this question.

Despite these limitations, FEA revealed interesting information regarding the mechanics of sacroplasty. Most notably, these data suggest that injection of PMMA into a fractured sacrum may decrease maximal principal stress and micromotion at the site of fracture propagation. Indeed, even a small point fusion of bone, as in the present model, may produce marked effects on bone stress and micromotion. FEA also suggested that maximal principal stress is attenuated more effectively when PMMA is injected relatively more proximal to the origin of the fracture. This finding is not surprising when considering the mechanics of the present sacral fracture model. In this model, sacral bone on 1 side of the fracture was fixed in space to approximate a 1-legged stance, whereas bone on the other side of the fracture was mobile. This system, therefore, would be expected to behave in a manner consistent with a lever arm, in which force is applied to produce torque. When force is applied to the mobile section of bone in the model, torque is experienced at the site of fracture propagation, thus producing stress. The area of cement fixation produced by sacroplasty resists this torque by effectively decreasing the length of the lever arm. Such mechanical data regarding changes in maximal principal stress following different fusion areas demonstrate the utility of FEA for investigating the structural properties of sacroplasty. Indeed, additional FEA simulations may help to further optimize sacroplasty, thus improving the safety and efficacy of this procedure.

The present FEA data build on previous FEA findings of decreased strain about idealized PMMA placement in a model of the intact sacrum.[14] Furthermore, the present data are consistent with similar findings of decreased fracture micromotion following vertebroplasty.[19] If fracture stress and micromotion contribute to pain associated with sacral fractures, then the present data may help to explain the apparent favorable clinical outcomes of sacroplasty. It is important to note, however, that the role of the placebo effect as an explanation for the apparent beneficial clinical outcomes of sacroplasty cannot be underestimated. Indeed, only a controlled prospective randomized trial could accurately establish the clinical efficacy of sacroplasty, beyond the nonspecific effects of placebo.[40]

Conclusion

Bone PMMA injections have become part of the expertise of neuroradiologists. As such, the development and expansion of the application of these techniques will likely be driven by this subspecialty of radiology. The present study demonstrates that sacral landmarks can be used with image guidance to safely place PMMA where sacral insufficiency fractures occur. In addition, this study suggests that FEA can provide valuable insight regarding the mechanical properties of PMMA injection

into sacral bone. FEA data suggest that the PMMA-bone interface may decrease maximal principal stress and micromotion at the site of sacral fracture propagation. Such favorable biomechanical characteristics may contribute to subjective patient reports of decreased pain and increased mobility following sacroplasty.

References

1. Lourie H. **Spontaneous osteoporotic fracture of the sacrum: an unrecognized syndrome of the elderly.** *JAMA* 1982;248:715–17
2. Lin J, Lachmann E, Nagler W. **Sacral insufficiency fractures: a report of two cases and a review of the literature.** *J Womens Health Gend Based Med* 2001;10:699–705
3. Grasland A, Pouchot J, Mathieu A, et al. **Sacral insufficiency fractures: an easily overlooked cause of back pain in elderly women.** *Arch Intern Med* 1996;156:668–74
4. Babayev M, Lachmann E, Nagler W. **The controversy surrounding sacral insufficiency fractures: to ambulate or not to ambulate?** *Am J Phys Med Rehabil* 2000;79:404–09
5. Lin JT, Lane JM. **Sacral stress fractures.** *J Womens Health* 2003;12:879–88
6. Garant M. **Sacroplasty: a new treatment for sacral insufficiency fracture.** *J Vasc Interv Radiol* 2002;13:1265–67
7. Pommersheim W, Huang-Hellinger F, Baker M, et al. **Sacroplasty: a treatment for sacral insufficiency fractures.** *AJNR Am J Neuroradiol* 2003;24:1003–07
8. Butler CL, Given CA 2nd, Michel SJ, et al. **Percutaneous sacroplasty for the treatment of sacral insufficiency fractures.** *AJR Am J Roentgenol* 2005;184:1956–59
9. Mattern CWT, Whitlow CT, Mussat-Whitlow BJ, et al. **Sacroplasty versus vertebroplasty: comparable clinical efficacy for the treatment of fracture-related pain.** Paper presented at: Annual meeting of the American Society of Neuroradiology, May 6–12, 2006; San Diego, Calif
10. Yoganandan N, Kumaresan S, Voo L, et al. **Finite element applications in human cervical spine modeling.** *Spine* 1996;21:1824–34
11. van Rietbergen B, Weinans H, Huiskes R. **Prospects of computer models for the prediction of osteoporotic bone fracture risk.** *Stud Health Technol Inform* 1997;40:25–32
12. Borah B, Gross GJ, Dufresne TE, et al. **Three-dimensional microimaging (MR-microI and microCT), finite element modeling, and rapid prototyping provide unique insights into bone architecture in osteoporosis.** *Anat Rec* 2001;265:101–10
13. Ezquerro F, Simon A, Prado M, et al. **Combination of finite element modeling and optimization for the study of lumbar spine biomechanics considering the 3D thorax-pelvis orientation.** *Med Eng Phys* 2004;26:11–22
14. Anderson DE, Cotton JR. **Mechanical analysis of percutaneous sacroplasty using CT image based finite element models.** *Med Eng Phys* 2007;29:316–25. Epub 2006 May 24
15. Rice JC, Cowin SC, Bowman JA. **On the dependence of the elasticity and strength of cancellous bone on apparent density.** *J Biomech* 1988;21:155–68
16. Giddings VL, Kurtz SM, Jewett CW, et al. **A small punch test technique for characterizing the elastic modulus and fracture behavior of PMMA bone cement used in total joint replacement.** *Biomaterials* 2001;22:1875–81
17. Jensen ME, Evans AJ, Mathis JM, et al. **Percutaneous polymethylmethacrylate vertebroplasty in the treatment of osteoporotic vertebral body compression fractures: technical aspects.** *AJNR Am J Neuroradiol* 1997;18:1897–904
18. Jensen ME, Dion JE. **Vertebroplasty relieves osteoporosis pain.** *Diagn Imaging* 1997;19:71–72
19. Mathis JM, Barr JD, Belkoff SM, et al. **Percutaneous vertebroplasty: a developing standard of care for vertebral compression fractures.** *AJNR Am J Neuroradiol* 2001;22:373–81
20. Kallmes DF, Schweickert PA, Marx WF, et al. **Vertebroplasty in the mid- and upper thoracic spine.** *AJNR Am J Neuroradiol* 2002;23:1117–20
21. Kallmes DF, Jensen ME. **Percutaneous vertebroplasty.** *Radiology* 2003;229:27–36
22. Hide IG, Gangi A. **Percutaneous vertebroplasty: history, technique and current perspectives.** *Clin Radiol* 2004;59:461–67
23. Nussbaum DA, Gailloud P, Murphy K. **A review of complications associated with vertebroplasty and kyphoplasty as reported to the Food and Drug Administration medical device related web site.** *J Vasc Interv Radiol* 2004;15:1185–92
24. Guglielmi G, Andreula C, Muto M, et al. **Percutaneous vertebroplasty: indications, contraindications, technique, and complications.** *Acta Radiol* 2005;46:256–68
25. Trout AT, Gray LA, Kallmes DF. **Vertebroplasty in the inpatient population.** *AJNR Am J Neuroradiol* 2005;26:1629–33
26. Laredo JD, Hamze B. **Complications of percutaneous vertebroplasty and their prevention.** *Semin Ultrasound CT MR* 2005;26:65–80
27. Kaufmann TJ, Wald JT, Kallmes DF. **A technique to circumvent subcutaneous cement tracts during percutaneous vertebroplasty.** *AJNR Am J Neuroradiol* 2004;25:1595–96
28. Smith DK, Dix JE. **Percutaneous sacroplasty: long-axis injection technique.** *AJR Am J Roentgenol* 2006;186:1252–55
29. Brook AL, Mirsky DM, Bello JA. **Computerized tomography guided sacroplasty: a practical treatment for sacral insufficiency fracture.** *Spine* 2005;30:450–54
30. Huiskes R, Chao EY. **A survey of finite element analysis in orthopedic biomechanics: the first decade.** *Biomech* 1983;16:385–409
31. Huiskes R, Hollister SJ. **From structure to process, from organ to cell: recent developments of FE-analysis in orthopaedic biomechanics.** *J Biomech Eng* 1993;115:520–27
32. Polikeit A, Nolte LP, Ferguson SJ. **The effect of cement augmentation on the load transfer in an osteoporotic functional spinal unit: finite-element analysis.** *Spine* 2003;28:991–96
33. Baroud G, Nemes J, Heini P, et al. **Load shift of the intervertebral disc after a vertebroplasty: a finite-element study.** *Eur Spine J* 2003;12:421–26
34. Keller TS, Kosmopoulos V, Lieberman IH. **Vertebroplasty and kyphoplasty affect vertebral motion segment stiffness and stress distributions: a microstructural finite-element study.** *Spine* 2005;30:1258–65
35. Kosmopoulos V, Keller TS. **Damage-based finite-element vertebroplasty simulations.** *Eur Spine J* 2004;13:617–25
36. Wilcox RK. **The biomechanics of vertebroplasty: a review.** *Proc Inst Mech Eng [H]* 2004;218:1–10
37. Sun K, Liebschner MA. **Evolution of vertebroplasty: a biomechanical perspective.** *Ann Biomed Eng* 2004;32:77–91
38. Bergmann G, Graichen F, Rohlmann A. **Hip joint loading during walking and running, measured in two patients.** *J Biomech* 1993;26:969–90
39. Pedersen DR, Brand RA, Davy DT. **Pelvic muscle and acetabular contact forces during gait.** *J Biomech* 1997;30:959–65
40. Turner JA, Deyo RA, Loeser JD, et al. **The importance of placebo effects in pain treatment and research.** *JAMA* 1994;271:1608–14